THE JOURNAL OF PHYSICAL CHEMISTRY Letters

Letter

pubs.acs.org/JPCL

Direct Characterization of Metal−Metal Bonds between Nuclei with Strong Quadrupolar Interactions via NMR Spectroscopy

Frédéric A. Perras and David L. Bryce*

Department of Chemistry and CCRI, University of Ottawa, 10 Marie Curie Pvt. D'Iorio Hall, Ottawa, Ontario K1N6N5, Canada

Supporting Information

ABSTRACT: Metal−metal bonds can be difficult to characterize directly. We demonstrate that J couplings between metal nuclei experiencing strong quadrupolar interactions can be easily measured from well-defined splittings in NMR spectra of powdered samples. Using $^{69/71}$Ga NMR, it is shown that homonuclear J coupling, which is four orders of magnitude smaller than the quadrupolar coupling in a series of compounds featuring gallium−gallium bonds, can be extracted with a 2-D NMR experiment. The dependence of the multiplets on crystal symmetry reveals information on the structures of two Ga−Ga-bonded compounds for which diffraction data are unavailable. Interpretation of the data in a molecular orbital framework provides insight into the nature of the metal−metal bond.

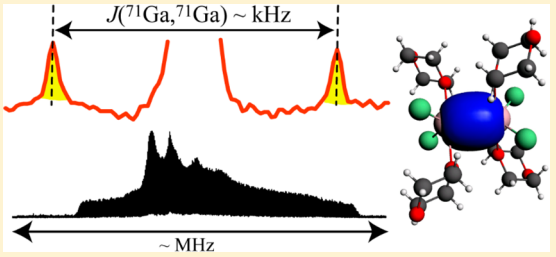

SECTION: Spectroscopy, Photochemistry, and Excited States

The characterization of metal−metal bonds, which are of fundamental importance in chemistry and catalysis, is commonly carried out via diffraction experiments in conjunction with theoretical calculations.[1−5] A particularly valuable experimental probe of chemical bonds is the J coupling between nuclear spins, which leads to the formation of characteristic multiplets in NMR spectra and is used to generate through-bond correlation spectra such as the familiar COSY and HMQC experiments.[6,7] Unfortunately, the measurement of J coupling across metal−metal bonds has been impeded by the fact that most metal nuclei are quadrupolar (spin $I > 1/2$). The quadrupolar nature of the NMR active isotopes, along with the strong electric field gradient (EFG) generated by the metal−metal bond, leads to NMR spectral line shapes that are often broadened beyond detection in solution or in powdered samples to such an extent that the effects of the relatively weak J coupling interaction are invisible. Additionally, for many such systems, the size of the quadrupolar interaction is such that the entire NMR spectrum of a powdered sample cannot be acquired in a single piece.[8] These broad lines have, to date, limited experimental studies to the recording of only 1-D NMR spectra. Spiess' beautiful pioneering studies of metal−metal bonds via NMR relied on single-crystal samples and provided insight from the EFG tensors and chemical shift anisotropy.[9] We report here the implementation of a simple shifted echo 2-D solid-state NMR method that enables the detection of spin−spin coupling between metal nuclei that are subject to very strong quadrupolar interactions in powders. The experiment requires only a single rf transmitter offset and provides definitive evidence of the presence of a metal−metal bond as well as insight into its electronic structure.

Ga−Ga bonded compounds comprise a particularly interesting class.[10,11] Gallium metal−metal-bonded systems have notably demonstrated that the bonding that is observed for the lighter main group elements is not necessarily representative of the heavier elements. For example, compounds featuring nonlinear Ga−Ga triple bonds that are weaker than the corresponding double bonds have been prepared.[12−14] Ga−Ga-bonded systems also provided the first example of all-metal aromaticity,[15,16] and many systems exhibit σ-aromaticity.[17,18] The simplest Ga−Ga-bonded systems are formed by dissolving gallium dichloride in a coordinating solvent such as dioxane.[19−21] Unlike $GaCl_2$, which has mixed monovalent and trivalent gallium sites,[22,23] the coordinated gallium dichloride compounds feature divalent Ga−Ga bonded sites; the dioxane salt is often used as a source of Ga(II).

We have prepared three Ga−Ga-bonded compounds, $Ga_2Cl_4(dioxane)_2$ (**1**), $Ga_2Cl_4(THP)_2$ (**2**), and $Ga_2Cl_4(THF)_2$ (**3**); see Chart 1. Two polymorphs are known for **1**: when it is crystallized at 0 °C, it forms dimeric, ethane-like molecules,[19] whereas when it is crystallized at room temperature it forms a

Chart 1. Ga−Ga-Bonded Compounds

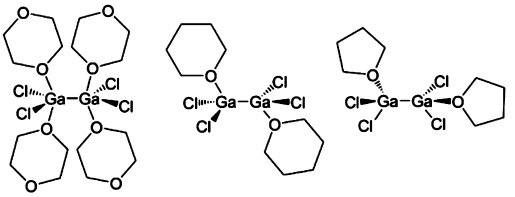

1 **2** **3**

Received: November 4, 2014
Accepted: November 7, 2014
Published: November 7, 2014

   dx.doi.org/10.1021/jz5023448 | J. Phys. Chem. Lett. 2014, 5, 4049−4054

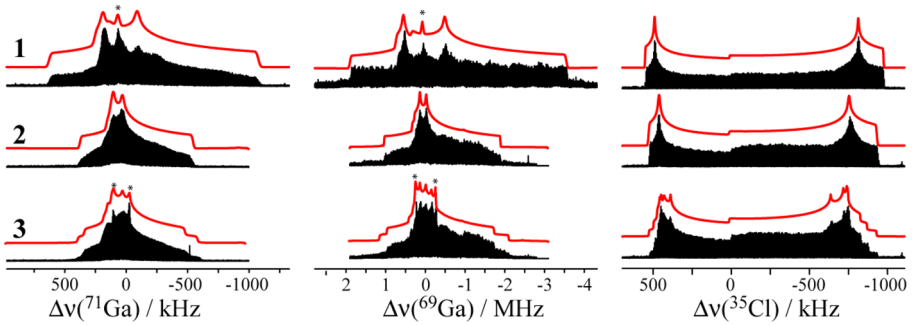

Figure 1. ^{71}Ga, ^{69}Ga, and ^{35}Cl WURST-QCPMG NMR spectra (21.1 T) for stationary powdered samples of **1** (top), **2** (middle), and **3** (bottom). The experimental spectra are shown in black, and the QUEST simulations are overlaid in red. Asterisks denote small impurity resonances in **1** and **3**; spectral modeling and elemental analysis confirm that the impurity level is ∼1% (see Supporting Information).

polymeric series of five-coordinate gallium dimers interconnected by dioxane ligands (see Chart 1).[21] The crystal structures for the other two compounds are unknown; however, the presence of a Ga−Ga bond has been inferred from Raman spectroscopy for both.[20] The purity of the compounds was confirmed by Ga and Cl ICP-MS elemental analysis and ^{13}C MAS NMR (Supporting Information).

The ultrawideline $^{69/71}$Ga and ^{35}Cl (all are spin-3/2 nuclides) NMR spectra of powdered samples of **1**, **2**, and **3** were acquired using the WURST-QCPMG pulse sequence[24] in a magnetic field of 21.1 T (see Figure 1). Even at such a high magnetic field strength, the central transition (CT) NMR spectra span over a megahertz, and it was necessary to acquire the full spectra in multiple pieces. The line shapes were simulated exactly using QUEST software,[25] and the simulation parameters are given in Table 1.

Table 1. ^{71}Ga and ^{35}Cl Chemical Shifts and Quadrupolar Parameters

compound	site	δ_{iso}/ppm	$\lvert C_Q\rvert$/MHz	η
1	Ga	200 ± 50	46.0 ± 0.5	0.75 ± 0.02
	Cl	100 ± 50	31.0 ± 0.1	0.09 ± 0.01
2	Ga	250 ± 50	32.8 ± 0.5	0.90 ± 0.02
	Cl	100 ± 50	30.2 ± 0.1	0.11 ± 0.01
3	Ga1	250 ± 50	35.5 ± 0.5	0.80 ± 0.02
	Ga2	250 ± 50	31.4 ± 0.5	0.90 ± 0.02
	Cl1	100 ± 50	27.4 ± 0.2	0.08 ± 0.02
	Cl2	100 ± 50	28.9 ± 0.2	0.07 ± 0.02
	Cl3	100 ± 50	29.5 ± 0.2	0.08 ± 0.02
	Cl4	100 ± 50	30.1 ± 0.2	0.11 ± 0.02

The gallium chemical shifts for these Ga(II) compounds (200 to 250 ppm) are consistent with the +2 oxidation state. The known chemical shift ranges for Ga(III) and Ga(I) sites are of 700 to 0 ppm and 0 to −700 ppm, respectively.[23,26−29] We are unaware of any previous reports of $^{69/71}$Ga NMR spectra for diamagnetic Ga(II) compounds. It can also be observed that the quadrupolar interaction at these gallium sites is much larger than what is typically found for Ga(I) or Ga(III) sites.[23,26,30] The quadrupolar coupling constant (C_Q(^{71}Ga)) for **1** is also noticeably larger than the values obtained for **2** and **3**, as is also evident qualitatively from the breadth of the powder patterns in Figure 1. This suggests that five-coordinate gallium sites are present in **1** rather than more symmetrical tetrahedrally coordinated gallium sites. This observation is consistent only with the polymeric polymorph of **1** because the dimeric polymorph features only four-coordinate gallium sites.[19] Compounds **2** and **3** cannot form such polymeric structures because THP and THF are monodentate ligands; these possess monomeric ethane-like structures and four-coordinate gallium sites.[19] The lower C_Q(^{71}Ga) values for **2** and **3** are consistent with such structures.

The C_Q(^{35}Cl) values of 27.4 to 31.0 MHz and near-axial symmetry of the ^{35}Cl EFG tensor ($\eta \approx 0$) are consistent with those of terminal chlorine sites and are in agreement with the molecular structures drawn in Chart 1.[23] It was also possible to resolve four separate low-frequency edges in the ^{35}Cl NMR spectrum of **3**, indicating that the four chlorine sites in the molecule are crystallographically inequivalent. This compound also has two inequivalent gallium sites, as seen in the $^{69/71}$Ga NMR spectra. Because of the symmetry of **1**, only a single gallium and chlorine site are expected; however, it is surprising that there is only a single gallium and chlorine site observed for **2** because its dioxane analogue, whose crystal structure is known,[19] does not have any particular symmetry.

While the previously described spectral analyses provide useful coordination information, they do not provide any direct insight into the Ga−Ga bond. We have recently shown that valuable, unambiguous information about the crystallographic symmetry of a molecule can be obtained from homonuclear *J*-resolved magic-angle spinning (MAS) NMR experiments on quadrupolar spin pairs.[31−33] These experiments yield a simple doublet for each pair of bonded atoms. The doublet splitting is amplified if there is inversion symmetry relating the two coupled atoms from *J* to 3*J* for spin-3/2 nuclei such as ^{71}Ga due to state mixing.[34] However, such MAS experiments cannot be performed in cases where the quadrupolar interaction results in CT powder patterns spanning more than the available MAS rate (MHz vs tens of kHz). Unfortunately, those are precisely the cases encountered for the vast majority of quadrupolar metal isotopes of interest. In those general cases, one is limited to performing NMR experiments on stationary powder samples[8] for which 2D NMR experiments are impractical or atypical. We have designed a shifted-echo 2-pulse *J*/*D*-resolved NMR experiment, reminiscent of the SEDOR and DEER experiments,[35,36] which can be used to obtain 2D NMR spectra for samples that yield ultrawideline 1-D NMR spectra (see Figure 2). Because there is no double-quantum filter, the *J*/*D*-resolved spectra will always feature a large peak at zero frequency that originates from ^{71}Ga sites coupled to ^{69}Ga, a satellite transition of ^{71}Ga, or a crystallite in a part of the powder pattern that is outside the bandwidth of the pulses. The use of a simple two-pulse experiment, however, has a greater

dx.doi.org/10.1021/jz5023448 | J. Phys. Chem. Lett. 2014, 5, 4049−4054

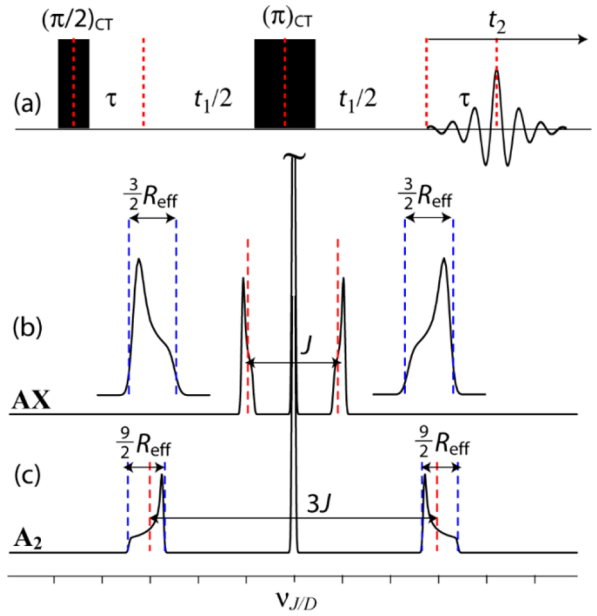

Figure 2. Shifted-echo *J*/*D*-resolved NMR pulse sequence (a) and the resulting theoretical spectra for the AX (b) and A_2 (c) cases (quadrupolar spin pairs in stationary powdered samples). Note the inversion of the sense of the line shapes in the AX compared with the A_2 case. Insets in panel b are enlarged. The theoretical spectra were simulated using WSolids' Static: Dipolar-chemical shift AX module[40] and the size and signs of *J* and R_{DD} were altered as described in the text for the A_2 case.

sensitivity, a wider excitation bandwidth, and greater resolution because the shifted echo ensures that absorptive line shapes are obtained.

Both the *J* and dipolar coupling interactions affect the *J*/*D*-resolved NMR spectra. The modulation frequency in the indirect dimension is given by $\pm(J/2 + d/2)$ when the sites are magnetically inequivalent (AX or AA′ spin system), as is the case for pairs of spin-1/2 nuclei. The dipolar modulation strength $(d = -R_{eff}(3\cos^2\theta - 1))$ depends on the angle between the Ga−Ga bond and the applied magnetic field (θ) and the effective dipolar coupling constant ($R_{eff} = R_{DD} - \Delta J/3$, where R_{DD} is the dipolar coupling constant and ΔJ is the anisotropy of the *J* coupling tensor).

When the spins are magnetically equivalent, however, the eigenstates of relevance to the CT take the following form; magnetic equivalence means identical NMR tensor magnitudes and orientations

$$\langle 1| = \langle 1/2,\ 1/2| \tag{1}$$

$$\langle 2| = \frac{1}{\sqrt{2}}(\langle -1/2,\ 1/2| + \langle 1/2,\ -1/2|) \tag{2}$$

$$\langle 3| = \langle -1/2,\ -1/2| \tag{3}$$

To calculate the *J*/*D*-resolved spectra it is then necessary to evaluate the impact of the *J*+*D* Hamiltonian on these states

$$\hat{H}_{D+J} = (J + d)\hat{I}_z\hat{S}_z + (J/2 - d/4)(\hat{I}_+\hat{S}_- + \hat{I}_-\hat{S}_+) \tag{4}$$

The two allowed CT transitions that would become modulated under a CT-selective Hahn echo[32] would then be affected by the spin−spin coupling interactions as follows

$$\langle 2|\hat{H}_{D+J}|2\rangle - \langle 1|\hat{H}_{D+J}|1\rangle = 3/2J - 3/2d \tag{5}$$

$$\langle 3|\hat{H}_{D+J}|3\rangle - \langle 2|\hat{H}_{D+J}|2\rangle = -3/2J + 3/2d \tag{6}$$

The modulation frequency in the indirect dimension of the 2-D experiment would then be equal to $\pm$ $(3J/2-3d/2)$ when the sites are magnetically equivalent (A_2 spin system); see the Supporting Information for more details. Simulated *J*/*D*-resolved NMR spectra are shown in Figure 2 for the AX and A_2 cases. In addition to showing clear spectral splittings of *J* or 3*J*, respectively, it can also be seen that the sense of the Pake-like powder patterns comprising each component of the doublet is reversed, providing an additional handle on the symmetry of the system. Note also that if the *J* coupling constant was negative, the sense of the powder patterns would also be reversed. With this simple 2D NMR approach, evidence of metal−metal bonding, information regarding the crystal symmetry, and insight into the electronic structure of the bond can be obtained simultaneously. This approach is also more sensitive, general, and easier to implement and interpret than other methods designed to measure dipolar coupling between quadrupolar nuclei.[37−39]

We have performed ^{71}Ga *J*/*D*-resolved NMR experiments on compounds **1** to **3**, and the resulting spectra are shown in Figure 3. Because of the limited bandwidth of the square rf

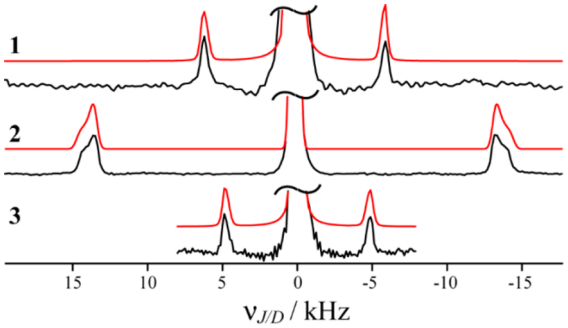

Figure 3. *J*/*D*-resolved ^{71}Ga NMR spectra (stationary powdered samples; B_0 = 21.1 T). Red: simulated; black: expt. The peak at zero frequency is truncated for clarity.

pulses, the 2D experiments are performed on only a single piece of the powder pattern (i.e., a single transmitter offset); the fact that the experiments can be done in this way opens the door to examining *J* couplings involving nuclei with enormous quadrupolar interactions. In all cases, the central part of the powder pattern with the highest intensity was used. Some spectra at various offsets were also acquired for **3** and were found to be consistent with the one displayed in Figure 3. Because the largest component of the Ga EFG tensor is expected to be aligned along the Ga−Ga bond and the η values are nearly equal to 1, both the perpendicular and parallel parts of the Pake-like powder patterns can be acquired at that offset, thus giving the full Pake powder pattern.[41] In principle, if the asymmetry parameter is closer to zero it would be necessary to perform two *J*/*D*-resolved experiments at the center and left edges of the CT powder pattern to acquire the full Pake line shape (see Supporting Information for more details).

It can be seen that for compound **2** the splitting is greatly amplified when compared with the other two samples. It is unreasonable to conclude that the larger splitting is caused by a much larger *J* coupling in this sample due to the structural similarity of the compounds. The key evidence that proves that the larger splitting observed for **2** must be 3*J* and not *J* is that

dx.doi.org/10.1021/jz5023448 | J. Phys. Chem. Lett. 2014, 5, 4049−4054

the powder patterns are oriented as required for the A_2 case. The sense of the powder patterns for **1** and **3** are as expected for an AX or AA′ spin system. It can then be concluded that the gallium sites in **2** are magnetically equivalent and that the molecule must have an inversion center. Although the Ga sites in **1** are related by two C_2 axes,[19] they do not share the same tensor orientations and they comprise an AA′ spin system for which the splitting is not amplified.

The *J*/*D*-resolved NMR experiment therefore not only establishes the ethane-like structure of $Ga_2Cl_4(THP)_2$ (**2**), whose crystal structure is unknown, but also makes it possible to determine that the molecule must adopt a staggered conformation with an inversion center, as depicted in Chart 1. This conclusion is also in agreement with the single ^{35}Cl, $^{69/71}Ga$, and ^{13}C resonances that were observed, consistent with high symmetry. We can also conclude that the molecular conformation of $Ga_2Cl_4(THF)_2$ (**3**) is eclipsed, as in the $Ga_2Cl_4(dioxane)_2$ dimer polymorph[19] because there is no inversion symmetry and there are two distinct gallium sites and four distinct chlorine sites.

The measured *J* coupling constants listed in Table 2 are significantly larger than the direct dipolar coupling constants (~800 Hz) for digallium compounds.[19] The reduced *J* coupling constants (*K*) are also much larger than those measured for the lightest icosagen, boron (*K*(B,B) values are ~80 × 10^{19} N A^{-2} m^{-3} whereas *K*(Ga,Ga) values are around 9000 × 10^{19} N A^{-2} m^{-3}; $K = 4\pi^2 J/\gamma_1\gamma_2 h$).[31] This is in agreement with the periodic trend that reduced coupling constants are larger for the heavier elements in a particular group of the periodic table.[42] The magnitude of $J(^{71}Ga,^{71}Ga)$ is also well reproduced by hybrid DFT calculations (Table 2). It is interesting to also note that the *J* coupling for **1** is significantly larger than for **2** and **3**, indicating that $J(^{71}Ga,^{71}Ga)$ is very sensitive to the geometry and electronic structure of the Ga−Ga bond. The same cannot be said of the ^{71}Ga chemical shifts because of the relatively low precision obtainable from such broad NMR powder patterns (Table 1).

Table 2. $J(^{71}Ga,^{71}Ga)$ Coupling Constants

compound	J_{iso}^{expt}/kHz	J_{iso}^{B3LYP}/kHz	ΔJ^{expt}/kHz[a]	ΔJ^{B3LYP}/kHz
1	12.0 ± 0.3	10.42	1.5 ± 0.7	1.21
2	9.2 ± 0.1	8.10	1.5 ± 0.2	1.18
3	9.6 ± 0.3	8.13	1.5 ± 0.7	1.18

[a]These values assume a R_{DD} value of 800 Hz.

To obtain a greater insight into the origins of this large *J* coupling, we additionally decomposed the DFT-computed $J(^{71}Ga,^{71}Ga)$ values in terms of natural localized molecular orbital (NLMO)[43] contributions. These calculations revealed that essentially the entire isotropic *J* coupling originates from the Ga−Ga *σ*-bonding NLMO (depicted in Figure 4). The measured *J* coupling may then be of use as a direct probe of this particular orbital. For example, it has recently been shown that this equivalent NLMO is responsible for the *J* coupling between boron atoms in diboron systems and that the *J* coupling value provides a direct probe of the orbital energy of the B−B *σ* bond.[33] In this case, with the heavier icosagen gallium, the DFT calculations also predict a lower NBO orbital energy (by 0.036 au) for the Ga−Ga bond in **1** when compared with the other samples, in agreement with its larger *J* coupling constant (see Supporting Information). This method could possibly then be used to characterize a wide range of different Ga−Ga bonding modes because the $J(^{71}Ga,^{71}Ga)$ values can be related to the energy, or form, of the metal−metal bond.

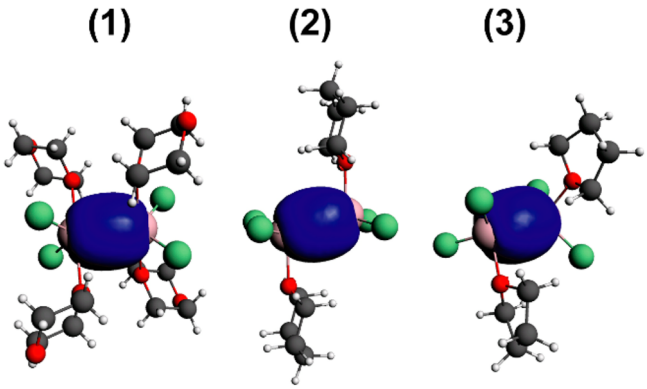

Figure 4. Ga−Ga *σ*-bonding NLMOs for the digallium compounds discussed in the text.

By fitting the fine structure of the *J*/*D*-resolved spectra, which is most evident for **2**, it is possible to extract an effective dipolar coupling constant of 300 Hz, which is significantly smaller than the expected dipolar coupling constant of 800 ± 50 Hz (from diffraction studies).[19] The difference is attributed to an anisotropy of the *J* coupling tensor of 1.5 kHz. This is only the third ΔJ value to be determined for a pair of quadrupolar nuclei using NMR and the first for a homonuclear spin pair.[34,44] The value is well reproduced using DFT calculations (see Table 2). In the case of lighter coupled nuclei, where ΔJ is much smaller than R_{DD}, the R_{eff} values would provide internuclear distance information. The DFT calculations predict that the *J* coupling tensor is axially symmetric and oriented along the internuclear axis, in agreement with the assumptions made in the analysis of the spectra.

We have demonstrated, using a 2-D NMR experiment, that it is possible to measure metal−metal *J* and dipolar coupling couplings that are four and five orders of magnitude smaller than the quadrupolar coupling constant, respectively. This makes it possible to access extremely valuable bonding information for samples whose 1-D NMR spectra show no direct evidence of these spin−spin couplings. The direct relationship between crystallographic symmetry and the fine structure of the NMR spectra also made it possible to elucidate the molecular structures and conformations of $Ga_2Cl_4(THP)_2$ and $Ga_2Cl_4(THF)_2$. The value of $J(^{71}Ga,^{71}Ga)$ is also shown to be a direct probe of the metal−metal *σ*-bond strength with the use of a NLMO analysis. This method can be applied to study a wide array of metal−metal bonded systems for which the *J* coupling was believed to be inaccessible due to the sheer magnitude of the quadrupolar interaction. This work also shows that samples yielding ultrawide 1-D NMR spectra are amenable to 2-D experiments that could yield valuable heteronuclear and homonuclear proximity information in, for example, metal−organic frameworks and heterogeneous catalysts.

■ ASSOCIATED CONTENT

Supporting Information

Synthetic and experimental details, elemental analyses, ^{13}C NMR data, DFT computations, NLMO analysis, and details of spectral simulations and their dependence on the tensor

dx.doi.org/10.1021/jz5023448 | J. Phys. Chem. Lett. 2014, 5, 4049−4054

orientations. This material is available free of charge via the Internet at http://pubs.acs.org.

AUTHOR INFORMATION

Corresponding Author

*E-mail: dbryce@uottawa.ca.

Notes

The authors declare no competing financial interest.

ACKNOWLEDGMENTS

We thank Dr. D. Richeson and Dr. V. Terskikh for useful discussions and Dr. N. De Silva for elemental analyses. We thank NSERC for funding. Access to the 900 MHz NMR spectrometer was provided by the National Ultrahigh-Field NMR Facility for Solids (www.nmr900.ca). Acknowledgment is made to the donors of The American Chemical Society Petroleum Research Fund for partial support of this research.

REFERENCES

(1) Cotton, F. A.; Harris, C. B. The Crystal and Molecular Structure of Dipotassium Octachlorodirhenate(III) Dihydrate, $K_2[Re_2Cl_8]2H_2O$. *Inorg. Chem.* **1965**, *4*, 330−333.

(2) Nguyen, T.; Sutton, A. D.; Brynda, M.; Fettinger, J. C.; Long, G. J.; Power, P. P. Synthesis of a Stable Compound with Fivefold Bonding Between Two Chromium(I) Centers. *Science* **2005**, *310*, 844−847.

(3) Brynda, M.; Gagliardi, L.; Widmark, P.-O.; Power, P. P.; Roos, B. O. A Quantum Chemical Study of the Quintuple Bond between Two Chromium Centers in [PhCrCrPh]: trans-Bent versus Linear Geometry. *Angew. Chem., Int. Ed.* **2006**, *45*, 3804−3807.

(4) Merino, G.; Donald, K. J.; D'Acchioli, J. S.; Hoffmann, R. The Many Ways to Have a Quintuple Bond. *J. Am. Chem. Soc.* **2007**, *129*, 15295−15302.

(5) Wagner, F. R.; Noor, A.; Kempe, R. Ultrashort Metal−Metal Distances and Extreme Bond Orders. *Nat. Chem.* **2009**, *1*, 529−536.

(6) Aue, W. P.; Bartholdi, E.; Ernst, R. R. Two-Dimensional Spectroscopy. Application to Nuclear Magnetic Resonance. *J. Chem. Phys.* **1976**, *64*, 2229−2246.

(7) Müller, L. Sensitivity Enhanced Detection of Weak Nuclei Using Heteronuclear Multiple Quantum Coherence. *J. Am. Chem. Soc.* **1979**, *101*, 4481−4484.

(8) Schurko, R. W. Ultra-Wideline Solid-State NMR Spectroscopy. *Acc. Chem. Res.* **2013**, *46*, 1985−1995.

(9) Spiess, H. W.; Sheline, R. K. Anisotropic Chemical Shifts in Trigonal Cobalt Carbonyls Containing Metal−Metal Bonds. *J. Chem. Phys.* **1970**, *53*, 3036−3041.

(10) Robinson, G. H. Gallanes, Gallenes, Cyclogallenes, and Gallynes: Organometallic Chemistry about the Gallium−Gallium Bond. *Acc. Chem. Res.* **1999**, *32*, 773−782.

(11) Robinson, G. H. On the organometallic chemistry of gallium and the dynamics of Ga−Ga bond formation. *Chem. Commun.* **2000**, 2175−2181.

(12) Su, J.; Li, X.-W.; Crittendon, R. C.; Robinson, G. H. How Short is a -Ga⋮Ga- Triple Bond? Synthesis and Molecular Structure of $Na_2[Mes^*_2C_6H_3\text{-}Ga⋮Ga\text{-}C_6H_3Mes^*_2]$ (Mes^* = 2,4,6-i-$Pr_3C_6H_2$): The First Gallyne. *J. Am. Chem. Soc.* **1997**, *119*, 5471−5472.

(13) Xie, Y.; Grev, R. S.; Gu, J.; Schaefer, H. F., III; Schleyer, P. v. R.; Su, J.; Li, X.-W.; Robinson, G. H. The Nature of the Gallium−Gallium Triple Bond. *J. Am. Chem. Soc.* **1998**, *120*, 3773−3780.

(14) Hardman, N. J.; Wright, R. J.; Phillips, A. D.; Power, P. P. Structures, Bonding, and Reaction Chemistry of the Neutral Organogallium(I) Compounds $(GaAr)_n$ (n = 1 or 2) (Ar = Terphenyl or Related Ligand): An Experimental Investigation of Ga−Ga Multiple Bonding. *J. Am. Chem. Soc.* **2003**, *125*, 2667−2679.

(15) Li, X.-W.; Pennington, W. T.; Robinson, G. H. Metallic System with Aromatic Character. Synthesis and Molecular Structure of $Na_2[[(2,4,6\text{-}Me_3C_6H_2)_2C_6H_3]Ga]_3$ The First Cyclogallane. *J. Am. Chem. Soc.* **1995**, *117*, 7578−7579.

(16) Boldyrev, A. I.; Wang, L.-S. All-Metal Aromaticity and Antiaromaticity. *Chem. Rev.* **2005**, *105*, 3716−3757.

(17) Twamley, B.; Power, P. P. Synthesis of the Square-Planar Gallium Species $K_2[Ga_4(C_6H_3\text{-}2,6\text{-}Trip_2)_2]$ (Trip=C_6H_2-2,4,6-iPr_3): The Role of Aryl−Alkali Metal Ion Interactions in the Structure of Gallium Clusters. *Angew. Chem., Int. Ed.* **2000**, *39*, 3500−3503.

(18) Kuznetsov, A. E.; Boldyrev, A. I.; Li, X.; Wang, L.-S. On the Aromaticity of Square Planar Ga_4^{2-} and In_4^{2-} in Gaseous $NaGa^{4+}$ and $NaIn^{4+}$ Clusters. *J. Am. Chem. Soc.* **2001**, *123*, 8825−8831.

(19) Beamish, J. C.; Small, R. W. H.; Worrall, I. J. Neutral Complexes of Gallium(II) Containing Gallium-Gallium Bonds. *Inorg. Chem.* **1979**, *18*, 220−223.

(20) Beamish, J. C.; Boardman, A.; Small, R. W. H.; Worrall, I. J. Neutral Complexes of Ga_2X_4 (X = Cl, Br) Containing Ga-Ga Bonds: The Crystal and Molecular Structure of Ga_2Cl_4·2Pyridine. *Polyhedron* **1985**, *4*, 983−987.

(21) Wei, P.; Li, X.-W.; Robinson, G. H. $[Ga_2Cl_4(dioxane)_2]_x$: Molecular Structure and Reactivity of a Polymeric Gallium(II) Halide Containing Two Five-Coordinate Gallium Atoms About a Ga−Ga Bond. *Chem. Commun.* **1999**, 1287−1288.

(22) Wilkinson, A. P.; Cheetham, A. K.; Cox, D. E. Study of Oxidation-State Contrast in Gallium Dichloride by Synchrotron X-Ray Anomalous Scattering. *Acta Crystallogr., Sect. B* **1991**, *47*, 155−161.

(23) Chapman, R. P.; Bryce, D. L. Application of Multinuclear Magnetic Resonance and Gauge-Including Projector-Augmented Wave Calculations to the Study of Solid Group 13 Chlorides. *Phys. Chem. Chem. Phys.* **2009**, *11*, 6987−6998.

(24) O'Dell, L. A.; Schurko, R. W. QCPMG Using Adiabatic Pulses for Faster Acquisition of Ultra-Wideline NMR Spectra. *Chem. Phys. Lett.* **2008**, *464*, 97−102.

(25) Perras, F. A.; Widdifield, C. M.; Bryce, D. L. QUEST-QUadrupolar Exact SofTware: a Fast Graphical Program for the Exact Simulation of NMR and NQR Spectra for Quadrupolar Nuclei. *Solid State Nucl. Magn. Reson.* **2012**, *45*−*46*, 36−44.

(26) McGarvey, B. R.; Taylor, M. J.; Tuck, D. G. Gallium-71 NMR Studies of Anionic Gallium Halide Species in Nonaqueous Solution. *Inorg. Chem.* **1981**, *20*, 2010−2013.

(27) Černy, Z.; Macháček, J.; Fusek, J.; Kříž, O.; Čásensky, B.; Tuck, D. G. ^{71}Ga NMR Studies of Mixtures of Gallium Trichloride and Trimethylgallium. *J. Organomet. Chem.* **1993**, *456*, 25−30.

(28) Massiot, D.; Vosegaard, T.; Magneron, N.; Trumeau, D.; Montouillout, V.; Berthet, P.; Loiseau, T.; Bujoli, B. ^{71}Ga NMR of Reference Ga_{IV}, Ga_V, and Ga_{VI} Compounds by MAS and QPASS, Extension of Gallium/Aluminum NMR Parameter Correlation. *Solid State Nucl. Magn. Reson.* **1999**, *15*, 159−169.

(29) Ash, J. T.; Grandinetti, P. J. Solid-state NMR Characterization of ^{69}Ga and ^{71}Ga in Crystalline Solids. *Magn. Reson. Chem.* **2006**, *44*, 823−831.

(30) Okuda, T.; Sato, M.; Hamamoto, H.; Ishihara, H.; Yamada, K.; Ichiba, S. Nuclear Quadrupole Resonance of 1,4-Dioxane Complexes with Gallium(II) and Gallium(III) Halides. *Inorg. Chem.* **1988**, *27*, 3656−3660.

(31) Perras, F. A.; Bryce, D. L. Symmetry-Amplified J Splittings for Quadrupolar Spin Pairs: A Solid-State NMR Probe of Homoatomic Covalent Bonds. *J. Am. Chem. Soc.* **2013**, *135*, 12596−12599.

(32) Perras, F. A.; Bryce, D. L. Theoretical Study of Homonuclear *J* Coupling Between Quadrupolar Spins: Single-Crystal, DOR, and J-Resolved NMR. *J. Magn. Reson.* **2014**, *242*, 23−32.

(33) Perras, F. A.; Bryce, D. L. Boron-Boron J Coupling Constants are Unique Probes of Electronic Structure: A Solid-State NMR and Molecular Orbital Study. *Chem. Sci.* **2014**, *5*, 2428−2437.

(34) Perras, F. A.; Bryce, D. L. Measuring Dipolar and J Coupling Between Quadrupolar Nuclei Using Double-Rotation NMR. *J. Chem. Phys.* **2013**, *138*, 174202.

(35) Kaplan, D. E.; Hahn, E. L. Expériences de Double Irradiation en Résonance Magnétique par la Méthode d'Impulsions. *J. Phys. Radium* **1958**, *19*, 821−825.

(36) Larsen, R. G.; Singel, D. J. Double Electron−Electron Resonance Spin−Echo Modulation: Spectroscopic Measurement of

Electron Spin Pair Separations in Orientationally Disordered Solids. *J. Chem. Phys.* **1993**, *98*, 5134−5146.
(37) Brinkmann, A.; Edén, M. Estimating Internuclear Distances Between Half-Integer Quadrupolar Nuclei by Central-Transition Double-Quantum Sideband NMR Spectroscopy. *Can. J. Chem.* **2011**, *89*, 892−899.
(38) Wi, S.; Logan, J. W.; Sakellariou, D.; Walls, J. D.; Pines, A. Rotary Resonance Recoupling for Half-Integer Quadrupolar Nuclei in Solid-State Nuclear Magnetic Resonance Spectroscopy. *J. Chem. Phys.* **2002**, *117*, 7024−7033.
(39) Wi, S.; Heise, H.; Pines, A. Reintroducing Anisotropic Interactions in Magic-Angle-Spinning NMR of Half-Integer Quadrupolar Nuclei: 3D MQMAS. *J. Am. Chem. Soc.* **2002**, *124*, 10652−10653.
(40) Eichele, K. *WSolids1*, version 1.20.15; University of Tübingen: Tübingen, Germany, 2011.
(41) Field, T. R.; Bain, A. D. Singularities in the Lineshape of a Second-Order Perturbed Quadrupolar Nucleus and Their Use in Data Fitting. *Solid State Nucl. Magn. Reson.* **2014**, *61−62*, 39−48.
(42) Bryce, D. L.; Wasylishen, R. E.; Autschbach, J.; Ziegler, T. Periodic Trends in Indirect Nuclear Spin-Spin Coupling Tensors: Relativistic Density Functional Calculations for Interhalogen Diatomics. *J. Am. Chem. Soc.* **2002**, *124*, 4894−4900.
(43) Autschbach, J. Analyzing Molecular Properties Calculated with Two-Component Relativistic Methods Using Spin-Free Natural Bond Orbitals: NMR Spin-Spin Coupling Constants. *J. Chem. Phys.* **2007**, *127*, 124106.
(44) Jakobsen, H. J.; Bildsøe, H.; Brorson, M.; Gan, Z.; Hung, I. Direct Observation of $^{17}O-^{185/187}Re$ ^{1}J-Coupling in Perrhenates by Solid-State ^{17}O VT MAS NMR: Temperature and Self-Decoupling Effects. *J. Magn. Reson.* **2013**, *230*, 98−110.